Giant resonances in ^{16}O

Y.-W. Lui, H. L. Clark, and D. H. Youngblood

Cyclotron Institute, Texas A&M University, College Station, Texas 77843

Giant resonances in ^{16}O have been studied with inelastic scattering of 240 MeV α particles at small angles. Isoscalar $E0$, $E1$, and $E2$ strength corresponding to $48\pm10\%$, $32\pm7\%$, and $53\pm10\%$, of the respective energy-weighted sum rule was identified between $E_x=11-40$ MeV with centroids of 21.13 ± 0.49, 21.67 ±0.61, and 19.76 ± 0.22 MeV and root-mean-square widths of 8.76 ± 1.82, 7.10 ± 0.52, and 5.11 ± 0.17 MeV, respectively. Elastic scattering and inelastic scattering to states at 6.13, 6.92, and 11.52 MeV were measured from $\theta_{c.m.}=2.5°$ to $11.5°$.

I. INTRODUCTION

The isoscalar giant monopole resonance (GMR) has been studied extensively between ^{12}C and ^{208}Pb [1–6]. Generally in heavier nuclei, close to 100% of $E0$ energy-weighted sum rule (EWSR) has been found [1], and most has been identified in lighter nuclei with 97% found in ^{40}Ca [7], 81% in ^{28}Si [8], and 72% seen in ^{24}Mg [4]. However, only 14.5% was located in ^{12}C [6]. ^{16}O is a doubly magic nucleus and has been the subject of several theoretical studies, however, there is no experimental data on the GMR. Therefore, it would be particularly interesting to measure the $E0$ strength distribution in ^{16}O. As 0° measurements required to enhance GMR strength eliminate using a conventional gas target due to scattering from windows, we have used a Mylar (contains H, C, and O) target and measured C also. The C contribution was then subtracted to obtain oxygen data. Isoscalar $E0$, $E1$, and $E2$ strength distributions for ^{16}O were then obtained.

II. EXPERIMENTAL TECHNIQUE AND RESULTS

A 240 MeV α-particle beam from the Texas A&M K500 superconducting cyclotron was used to bombard a 2.16 mg/cm^2 Mylar foil located in the target chamber of the multipole-dipole-multipole spectrometer. Inelastically scattered α particles were detected in a focal plane detector that measured position and angle in the scattering plane. The out-of-plane scattering angle ϕ was not measured. Position resolution of approximately 0.9 mm and scattering angle resolution of about 0.09° were obtained. The experimental technique and the detector have been described in detail in Ref. [4].

Giant resonance data were taken over the range $10 \leqslant E_x$ $\leqslant 55$ MeV with the spectrometer at 0° and at 4°, with the acceptance $\Delta\theta=\Delta\phi=4°$. C data were taken immediately after the Mylar data. Data were also taken with ^{24}Mg and ^{28}Si targets at 4° to obtain the energy calibration. Elastic and inelastic scattering data for discrete states were taken at spectrometer angles of 3.5°, 5.5°, and 7.5° at a higher dipole field setting with the vertical acceptance of the spectrometer reduced to ±0.8°. Each data set was divided into ten angle bins, each corresponding to $\delta\theta\approx0.4°$ using the angle obtained from ray tracing. ϕ is not measured by the detector, so the average angle for each bin was obtained by integrating

over the height of the solid angle defining slit and the width of the angle bin. Cross sections were obtained from the charge collected, target thickness, dead time, and known solid angle. Uncertainties in the subtraction process as well as target thickness, solid angle, etc., result in about a ±12% uncertainty in absolute cross sections.

Spectra of ^{16}O were obtained for each of the angle bins by subtracting the normalized C spectrum from the corresponding Mylar spectrum. The ^{16}O spectra obtained at two angles are shown in Fig. 1. The solid line in Fig. 1 indicates the choice of continuum underneath the giant resonance (GR)
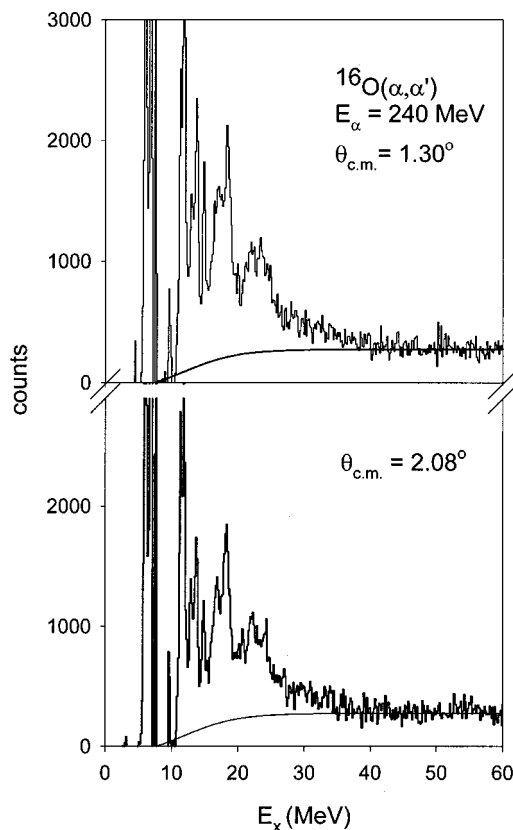

FIG. 1. Spectra obtained for ^{16}O(α,α') at $E_\alpha=240$ MeV for two angles. The average center-of-mass angles are indicated. The solid line indicates the division chosen between the GR peak and the continuum.
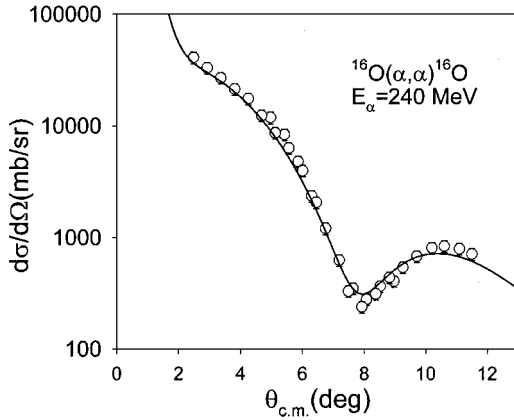
FIG. 2. Angular distribution of the differential cross section for elastic scattering of 240 MeV α particles from ^{16}O. The solid line shows the optical-model calculation. When not shown, statistical errors are smaller than the data points.

FIG. 3. (a) Angular distribution of the differential cross section for inelastic α particle scattering to the 6.13 meV 3^- state in ^{16}O. The solid line shows an $L=3$ DWBA calculation for $\beta R = 1.02$. (b) Angular distribution of the differential cross section for inelastic α particle scattering to the 6.92 MeV 2^+ state in ^{16}O. The solid line shows an $L=2$ DWBA calculation for $\beta R = 0.71$. (c) Angular distribution of the differential cross section for inelastic α scattering to the 11.52 MeV 2^+ state in ^{16}O. The solid line shows an $L=2$ DWBA calculation for $\beta R = 0.54$.

peak. The procedure used to determine the shape of the continuum was similar to that described in detail in Ref. [7]. The GR peak extends up to about $E_x = 40$ MeV, similar to that seen in other nuclei [4,5].

The angular distribution of the elastic scattering is shown in Fig. 2, while inelastic scattering to the 6.13 MeV 3^- state, 6.92 MeV 2^+ state, and the 11.52 MeV 2^+ state are shown in Fig. 3. The GR region ($11 < E_x < 40$ MeV) was divided into 477 keV energy intervals and the cross section was obtained for each interval both for the GR peak and the continuum. Angular distributions obtained for several energy intervals of the GR peak and the continuum are shown in Figs. 4 and 5, respectively.

III. DISTORTED-WAVE BORN APPROXIMATION (DWBA) ANALYSIS

The transition densities and the sum rules for various multipolarities are described thoroughly by Satchler [9]. The GMR has generally been considered a breathing mode oscillation and the corresponding transition density is given by [9]

$$U = -\alpha_0 \left[3\rho + r \frac{d\rho}{dr} \right],$$

where for a state that exhausts the EWSR

$$\alpha_0^2 = 2\pi \frac{\hbar^2}{mA\langle r^2 \rangle E_s}.$$

While the folding model provides more accurate cross sections for higher multipoles, it has been demonstrated that the deformed potential model and the folding model yield similar $0°$ cross sections and angular distributions for the GMR [3,10] if the potential deformation length is assumed to be equal to the mass deformation length ($\alpha_m c = \alpha_p R_p$). Elastic scattering data sufficient to determine optical model or folding parameters are not available for 240 MeV α par-
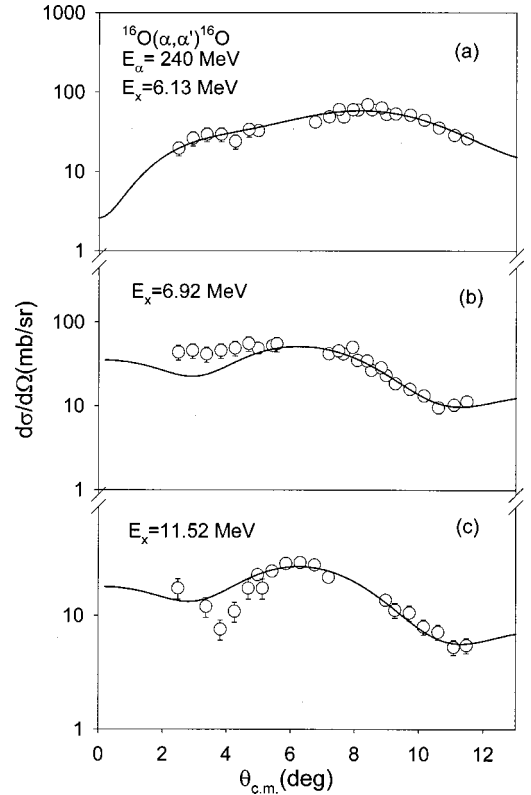
ticles on ^{16}O. Therefore, we have used optical-model parameters obtained for ^{28}Si [5] for a deformed potential analysis in this study.

Distorted-wave Born approximation and optical-model calculations were carried out with the code PTOLEMY [11]. Input parameters for PTOLEMY were modified [12] to obtain a correct relativistic calculation. Radial moments for ^{16}O were obtained by numerical integration of the Fermi mass distribution assuming $c = 2.413$ fm and $a = 0.523$ fm [13].

The optical-model calculation for elastic scattering is shown superimposed on the data in Fig. 2. The calculation is in reasonable agreement with the data. DWBA calculations for the 6.13 MeV 3^- state, the 6.92 MeV 2^+ state, and the 11.52 MeV 2^+ state normalized to the data are shown in Fig. 3. They are in reasonably good agreement with the data and the deformation lengths (βR) deduced are similar to those from other α, α' studies as can be seen in Table I. However, $B(E2)$ values obtained from the deformation lengths are smaller than those from electromagnetic measurements [14]. This is consistent with the conclusion of Beene, Horen, and Satchler [15] that deformed potential calculations result in $B(EL)$ values that can be a factor of 2 smaller than the electromagnetic values for 2^+ states. The cross section for
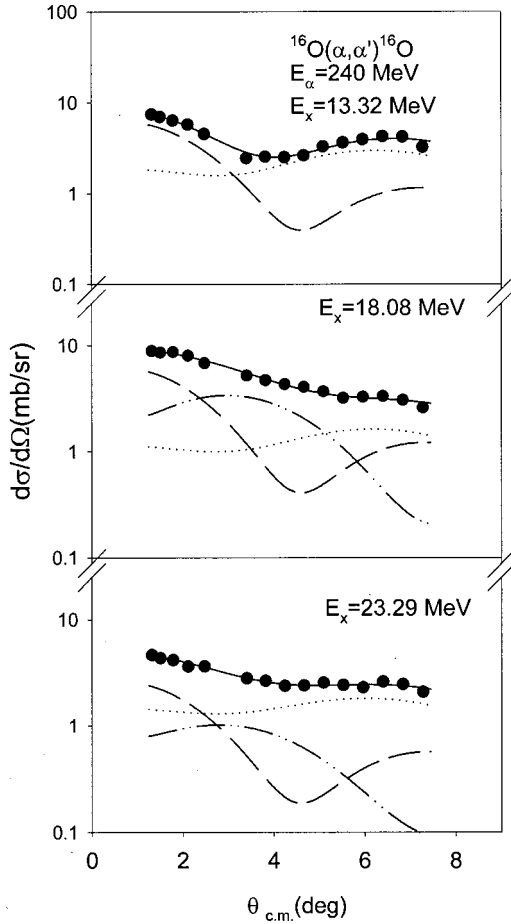
FIG. 4. Angular distributions of the differential cross section for inelastic α scattering for three excitation ranges of the GR peak in ^{16}O. The solid lines show the sum of the distributions for the individual multipolarities. The dashed lines show the $L=0$ component. The dash-dot-dot lines show the $L=1$ $T=0$ component. The dotted lines show the $L=2$ component.
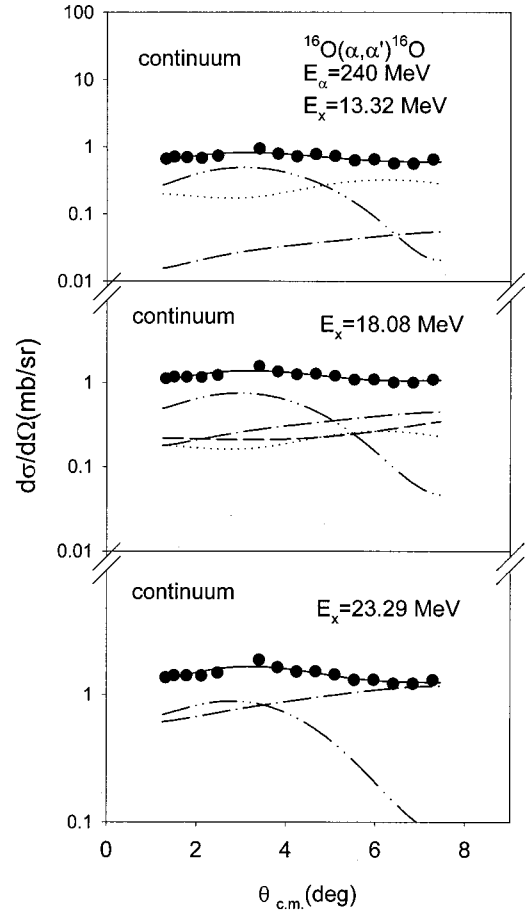
FIG. 5. Angular distributions of the differential cross section for inelastic α scattering for three excitation ranges of the continuum in ^{16}O. The solid lines show the sum of the distributions for the individual multipolarities. The dash-dot-dot lines show the $L=1$ $T=0$ component, the dotted lines show $L=2$ component, the dash-dot lines show $L=3$ component, and the short dashed line shows the $L=4$ component.

the 6.92 MeV 2^+ state is about a factor of 1.83 smaller than predicted using the electromagnetic value, therefore, all 2^+ strength was normalized by this factor. The deformation lengths extracted from the present work for discrete states and the fraction of the energy weighted sum rule obtained from the electromagnetic values are listed in Table I.

IV. DISCUSSION

Relativistic Hartree-Fock calculations [16] predicted significant $E0$ strength up to 45 MeV in ^{16}O, and $E0$ strength was found experimentally up through 35 MeV in ^{24}Mg [4] and ^{28}Si [5,8]. It is clearly important to investigate the strength distribution over as wide an excitation energy range as possible, especially for light nuclei. As shown in Fig. 1, there is clearly extra strength above a reasonable continuum choice up to $E_x=40$ MeV. Cross sections obtained in the GR data below $E_x=11$ MeV are not reliable as the solid angle changes due to cut offs in the detector; therefore, we have analyzed the region between $11 \leqslant E_x \leqslant 40$ MeV.

Angular distributions of the GR peak and the continuum

were fit with a sum of isoscalar 0^+, 1^-, 2^+, 3^-, and 4^+ strengths. The details of this slice analysis were described in Refs. [7,4]. Fits to angular distributions obtained for three excitation ranges of the GR peak and the continuum are shown in Figs. 4 and 5, respectively. $E0$, $E1$, and $E2$ strength distributions obtained from the analysis of the GR peak are shown in Fig. 6. Some of the apparent fragmentation in the higher excitation region may be because of relatively poor statistics due to the subtraction of C data over the entire excitation region. The parameters obtained are listed in Table II. Complete analyses with different normalizations in the subtraction process as well as different choices of the continuum were also carried out to estimate the uncertainties. Therefore, the errors include the uncertainties in cross section, the subtraction process, choice of continuum and fitting process. Although the uncertainties in the centroids are quite large, the accuracy of the energy calibration is approximately 50 keV, since the GR region was calibrated to the 13.88 MeV state in ^{24}Mg before and after each experimental run.

A total of $48\pm10\%$ of $E0$ EWSR is found in the region and about 15% of that is located between 30 and 40 MeV.

TABLE I. βR values obtained for low-lying states in ^{16}O.

E_x (MeV)	J^π	βR^a (fm)	EWSR^a (%)	βR^b (fm)	EWSR^b (%)	EWSR^c (%)
6.13	3^-	1.02	4.0		4.9	10.3
6.92	2^+	0.71	6.0	0.70	5.8	11.0
11.52	2^+	0.54	5.6	0.51	5.1	8.9

^{a}Present work.
^{b}Reference [19].
^{c}Reference [14].

Two narrow 0^+ peaks were identified at 11.96 and 13.93 MeV containing 2.3% and 3.5% of the $E0$ EWSR, respectively. In inelastic electron scattering, these peaks were found to contain 9.9% and 6.5% [17] of the $E0$ EWSR. No $E0$ strength was found in the continuum. The characteristic of the monopole is the strongly forward peaked angular distribution. The isovector giant dipole resonance is also forward peaked, but it is much weaker than the other multipolarities and has no impact on this analysis. This feature of the angular distribution is a unique signature of $E0$ strength even in the continuum [4,7], while strength distributions for other multipoles cannot reliably be obtained for the continuum.

Isoscalar $E1$ strength corresponding to $32 \pm 7\%$ of the $E1$ EWSR was found with a centroid of 21.67 ± 0.52 MeV and rms width of 7.10 ± 0.43 MeV. In general, the isoscalar $E1$ angular distribution fills in the first minimum of the isoscalar $E0$ angular distribution, thus the $E1$ results are more sensitive to the choice of continuum than the other multipolarities. However, in the different analyses used to estimate the errors, $E1$ strength varied from 29% to 34% with the centroid varying ± 0.52 MeV and hence was less sensitive than in the recent analysis of ^{40}Ca [7]. This is, in part, due to a low continuum and the fact that the angular distributions change more slowly with angle than those for the higher masses.

$E2$ strength corresponding to $53 \pm 10\%$ of the $E2$ EWSR was observed, mostly below $E_x = 30$ MeV as can be seen in Fig. 6. The centroid of the distribution is at 19.76 ± 0.22 MeV and the rms width is 5.11 ± 0.17 MeV. The 11.52 MeV state contained $9.4 \pm 1.5\%$ $E2$ EWSR, in excellent agreement with the $10.0 \pm 2.0\%$ extracted from the separate run measuring the elastic scattering and low-lying states. Within the errors the $E2$ strength is in agreement with the $81 \pm 30\%$ obtained by Knopfle et al. [18] and the 60% obtained by Harakeh et al. [19]. Note that these strengths result after applying the factor of 1.83 obtained for the 6.92 MeV 2^+ state. The $E3$ and $E4$ strength could not be separated
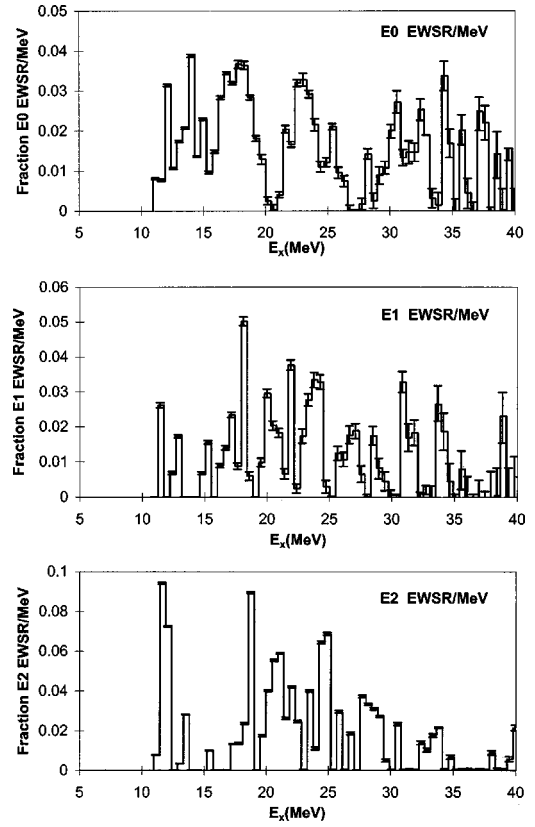

FIG. 6. Strength distributions obtained are shown by histograms. Error bars represent the uncertainty from the fitting of the angular distributions.

within the limited angle range of this experiment, but less than 20% of the EWSR was seen, with large uncertainties.

There are several theoretical calculations using different approaches and different methods to calculate the GMR in ^{16}O. Blaizot, Gogny, and Grammaticos [20] in 1976 used the random-phase approximation (RPA) and self-consistent wave functions with several Gogny interactions. More recently Vretenar et al. used time-dependent relativistic mean-field theory with various parameter sets to calculate the properties of GMR [21]. Ma et al. [16] used the framework of relativistic RPA with nonlinear terms in the calculation. Each of these relativistic models can correctly reproduce the energy of GMR for heavy nuclei, but some required a nuclear incompressibility much higher than the $K_{nm} = 231$ MeV required to fit the experimental GMR energies in heavy nuclei with the Gogny interaction [1]. Wang, Chung, and Santiago [22] using the nuclear Thomas-Fermi approximation, obtain a nuclear incompressibility of about 234 MeV. Using a linear

TABLE II. Parameters obtained for $E0$, $E1$, and $E2$ strength between $E_x = 11-40$ MeV in ^{16}O.

L	$\%E0$ EWSR (%)	m_1/m_0 (MeV)	$\sqrt{m_3/m_1}$ (MeV)	$\sqrt{m_1/m_{-1}}$ (MeV)	rms width (MeV)
0	48 ± 10	21.13 ± 0.49	24.89 ± 0.59	19.63 ± 0.38	8.76 ± 1.82
1	32 ± 7	21.67 ± 0.61			7.10 ± 0.52
2	53 ± 10	19.76 ± 0.22			5.11 ± 0.17

TABLE III. Comparison of GMR energies in ^{16}O.

m_1/m_0 (MeV)	$\sqrt{m_3/m_1}$ (MeV)	$\sqrt{m_1/m_{-1}}$ (MeV)	K_{nm} (MeV)	
21.13 ± 0.49	24.89 ± 0.59	19.63 ± 0.38		Present work
		24.6	228	Ref. [20]
25.30			281	Ref. [16]
22.60			272	Ref. [21]
	19.56		234	Ref. [22]
	24.60		240	Ref. [23]

scaling assumption, they obtain GMR energies slightly below the experimental values in heavy nuclei [1]. Nayak *et al.* employed the extended Thomas-Fermi approximation to calculate coefficients based on Skyrme type interactions. These coefficients are used in the modified Leptodermous expansion including higher-order terms to extract nuclear incompressibility [23]. The moments obtained for $E0$ strength in ^{16}O with interactions that give the best fit to heavier nuclei together with the nuclear matter incompressibility are shown in Table III.

The moment obtained by Nayak *et al.* [23] is in agreement with the experimental values while that obtained by Vretenar *et al.* [21] is slightly above the experimental value. On the other hand, the GMR energy for ^{16}O calculated by Wang, Chung, and Santiago [22] is much too low. Ma's [16] and Blaizot's [20] values are considerably higher than the experimental value. As we identify only about half the $E0$ strength, a comparison of centroid, etc. may be misleading as the missing strength is likely to be in the higher excitation region and the centroids of all of the strength might be quite different. However, we note that the $E0$ strength obtained by electron scattering for states at 12 and 14 MeV were about a factor of 4.3 and 1.9, respectively, higher than our results, which might imply our strength estimates are too low. If so, we may have seen all of the strength, and the centroid comparisons are valid. Then the result of Nayak *et al.* with the nonrelativistic RATP interaction and Vretenar *et al.* with a relativistic calculation and the $NL3$ interaction would best describe the mass dependence of the nuclear compressibility. Later relativistic RPA calculations have shown [24] that if the Dirac sea states are included, interactions with nuclear incompressibilities in the range of 250–270 MeV reproduce the GMR in heavy nuclei, but these calculations have not been extended to ^{16}O [24]. Blaizot *et al.*, in a 1995 calculation [25] that fits the mass dependence from $40<A<208$, also did not show results for ^{16}O.

Ma *et al.* [16] gave the calculated strength distribution for ^{16}O, and an actual comparison of the strength distributions could reveal whether disagreements are due to missing strength at higher excitation. The experimental $E0$ strength distribution was converted to a monopole response function and is compared to the relativistic RPA calculation using the TMI parameter set from Ma *et al.* [16]. The centroid they obtain is at 25.3 MeV, which is higher than the present experimental result by 4.2 MeV. They did not give the $E0$ EWSR for their distribution, but an estimate from their graph gives about 120%. We shifted their calculation by 4.2 MeV
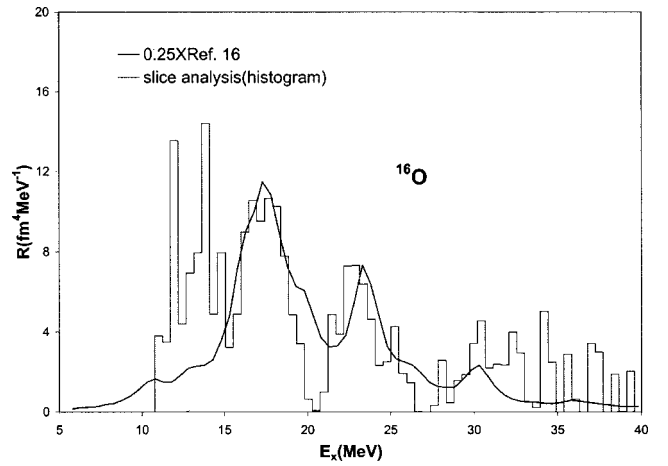

FIG. 7. The histogram is the experimental $E0$ strength converted to monopole response function. The black line shows the monopole response function from Ref. [16] multiplied by 0.25 and shifted by 4.2 MeV.

to match the experimental centroid and normalized their calculation to approximately 30% of $E0$ EWSR by multiplying the curve by a factor of 0.25 and the result is shown in Fig. 7. The normalized/shifted curve and the experimental result are in moderately good agreement on the shape of the gross structures, however, the calculation failed to predict the two 0^+ states found at 11.96 and 13.93 MeV in both this work and electron scattering [17].

There are several possible reasons our measurement yields only 48% of the $E0$ EWSR. The transition density used in DWBA calculations is the same as in heavy nuclei, whereas RPA calculations have suggested [26] that the transition density in light nuclei is quite different and this could have a significant effect on predicted cross sections. This could be tested if microscopic transition densities were available for ^{16}O. In heavier nuclei the deformed potential and folding model gave similar cross sections for $E0$ strength, but this might not be true in ^{16}O. Experimentally, the statistics on the present measurement at higher excitation are relatively poor because of the necessity for subtracting C data. Considerably better statistics might reveal more strength. Also if the $E0$ strength extends beyond $E_x=42$ MeV, it would be obscured by the ^{16}O($\alpha,\,^5$Li$\rightarrow\alpha+p$) reaction. A higher beam energy would move the contributions from this process higher in excitation.

V. CONCLUSIONS

The giant resonance region between 11 and 40 MeV in ^{16}O has been studied using 240 MeV α particles at small angles. Slice analysis was used to extract isoscalar strength with 477 keV resolution. Substantial strength for $L=0$, 1, and 2 has been located with strengths fragmented throughout the region. In ^{16}O, $48\pm10\%$ of the $E0$ EWSR was identified with a centroid of 21.13 ± 0.61 MeV. This is less strength than that observed in ^{24}Mg and ^{28}Si but substantially more than that seen in ^{12}C. If these results are normalized to electron scattering, then we have seen 90–200 % of the $E0$

EWSR. If the assumption is made that we have seen all of the $E0$ strength, then the nonrelativistic calculations of Nayak *et al.* using the RATP interaction with $K_{nm} = 240$ MeV best describe the GMR energies in both heavy nuclei and in ^{16}O and hence reproduce the compressibilities of finite nuclei over a wide range of A. The relativistic calculation of Ma *et al.* shows structure in the $E0$ distribution similar to the data, but approximately 4.2 MeV higher in excitation. A number of calculations of heavier nuclei using different interactions and approaches such as that by Blaizot *et al.* [25] have been carried out in recent years, but not for nuclei lighter than ^{40}Ca. Hopefully this data will stimulate such calculations for ^{16}O.

[1] D. H. Youngblood, H. L. Clark, and Y.-W. Lui, Phys. Rev. Lett. **82**, 691 (1999).

[2] Y.-W. Lui, H. L. Clark, and D. H. Youngblood, Phys. Rev. C **61**, 067307 (2000).

[3] D. H. Youngblood, Y.-W. Lui, and H. L. Clark, Phys. Rev. C **55**, 2811 (1997).

[4] D. H. Youngblood, Y.-W. Lui, and H. L. Clark, Phys. Rev. C **60**, 014304 (1999).

[5] D. H. Youngblood, H. L. Clark, and Y.-W. Lui, Phys. Rev. C **57**, 1134 (1998).

[6] D. H. Youngblood, Y.-W. Lui, and H. L. Clark, Phys. Rev. C **57**, 2748 (1998).

[7] D. H. Youngblood, Y.-W. Lui, and H. L. Clark, Phys. Rev. C **63**, 067301 (2001).

[8] D. H. Youngblood, Y.-W. Lui, and H. L. Clark (unpublished).

[9] G. R. Satchler, Nucl. Phys. **A472**, 215 (1987).

[10] G. R. Satchler and Dao T. Khoa, Phys. Rev. C **55**, 285 (1997).

[11] M. Rhondes-Brown, M. H. Macfarlane, and S. C. Pieper, Phys. Rev. C **21**, 2417 (1980); M. H. Macfarlane and S. C. Pieper, Argonne National Laboratory Report No. ANL-76-11, Rev. 1, 1978 (unpublished).

[12] G. R. Satchler, Nucl. Phys. **A540**, 533 (1992).

[13] G. Fricke, C. Bernhardt, K. Heilig, L. A. Schaller, L. Schellenberg, E. B. Shera, and C. W. DeJager, At. Data Nucl. Data Tables **60**, 177 (1995).

[14] F. Ajzenberg-Selove, Nucl. Phys. **A460**, 1 (1986), data extracted from the ENSDF database, version(90), NNDC.

[15] J. R. Beene, D. J. Horen, and G. R. Satchler, Phys. Lett. B **344**, 67 (1995).

[16] Z. Ma, N. Van Giai, H. Toki, and Marcelle L'Huillier, Phys. Rev. C **55**, 2385 (1997).

[17] M. W. Krison, Nucl. Phys. **A257**, 58 (1976).

[18] K. T. Knopfle, G. J. Wagner, H. Breuer, M. Rogge, and C. Mayer-Boricke, Phys. Rev. Lett. **35**, 779 (1975).

[19] M. N. Harakeh, A. R. Arends, M. J. A. De Voigt, A. G. Drentje, S. Y. van der Werf, and A. van der Woude, Nucl. Phys. **A265**, 189 (1976).

[20] J. P. Blaizot, D. Gogny, and B. Grammaticos, Nucl. Phys. **A265**, 315 (1976).

[21] D. Vretenar, G. A. Lalazissis, R. Behnsch, W. Poschl, and P. Ring, Nucl. Phys. **A621**, 853 (1997).

[22] C. S. Wang, K. C. Chung, and A. J. Santiago, Phys. Rev. C **55**, 2844 (1997).

[23] R. C. Nayak, J. M. Pearson, M. Farine, P. Gleissl, and M. Brack, Nucl. Phys. **A516**, 62 (1990).

[24] Zhong-Yu Ma, Nguyen Van Giai, A. Wandelt, D. Vretenar, and P. Ring, Nucl. Phys. **A686**, 173 (2001).

[25] J. P. Blaizot, J. F. Berger, J. Decharge, and M. Girod, Nucl. Phys. **A591**, 435 (1995).

[26] K. Goeke, Phys. Rev. Lett. **38**, 212 (1977).